ejpmr, 2019,6(9), 42-58

SJIF Impact Factor 4.897

EUROPEAN JOURNAL OF PHARMACEUTICAL AND MEDICAL RESEARCH

www.ejpmr.com

Research Article

ISSN 2394-3211

EJPMR

SYNTHESIS OF ORGANOTIN POLY(AMINE ETHERS) FROM THE HIV DRUG LAMIVUDINE (3TC)

Francesca Mosca,[1] Charles E. Carraher Jr.,[1*] Michael R. Roner,[2] Paul Slawek,[1] Alisa Moric-Johnson,[2] Lindsey C. Miller[2] and Jerome E. Haky[1]

[1]Florida Atlantic University, Department of Chemistry and Biochemistry, Boca Raton, FL 33431.
[2]University of Texas Arlington, Department of Biology, Arlington, TX 76010.

***Corresponding Author: Charles E. Carraher Jr.**

Florida Atlantic University, Department of Chemistry and Biochemistry, Boca Raton, FL 33431.

Article Received on 27/06/2019 **Article Revised on 18/07/2019** **Article Accepted on 07/08/2019**

ABSTRACT

Organotin poly(amine ethers) were rapidly synthesized in good yield employing the interfacial polycondensation system. Yield increases as the size of the alkyl group on the tin increases. Synthesis employed commercially available reactants allowing for ready production in gram to kilogram quantities. Infrared spectroscopy showed the formation of new bands characteristic of the Sn-O- and Sn-N linkages. MALDI MS shows ion fragment clusters to nine and ten units in length. The polymers exhibit decent inhibition of all of the tested human cancer cell lines including two human pancreatic, two human breast and two human glioblastoma brain cancer cell lines.

KEYWORDS: Organotin poly(amine ethers); HIV; lamivudine; MALDI MS; interfacial polymerization; pancreatic cancer; breast cancer; cancer; brain cancer; glioblastoma inhibition.

INTRODUCTION

We have synthesized a variety of organotin-containing polymers.[1] Currently, our emphasis is studying the structure-property relationship related to the ability of some of these polymers curtailing the growth of unwanted pathogens and infectious agents including cancers, viruses, bacteria, molds, and fungi. Some of this activity has been recently reviewed.[1-6] The general approach is to match Lewis acids that have known biological activities such as tin with Lewis bases that also exhibit known biological activities hoping for a synergetic effect.

Lamivudine (Fig. 1; also called 3TC) is a potent reverse transcriptase prodrug antiviral molecule employed in the treatment of AIDS.[7-9] Structurally, lamivudine is a nucleoside analogue. In HIV treatment it is administered several times daily because of its short half-life of 5-7 hours. It has additional problems including negative effects from the accumulation of the drug, high cost, and lack of patient compliance. Further, there is an increased incidence of co-infection of HIV with such diseases as tuberculosis. Co-treatments are being investigated. For instance, co-loaded polymer microspheres containing lamivudine and an anti tuberculosis drug such as isoniazid have been described that allow the treatment of both the HIV and tuberculosis.[10]

While lamivudine, Fig. 1, contains both a hydroxyl and amine group that can be employed incorporating it into polymers, this approach has not been widely used. Daniel and coworkers have synthesized a family of polymers based on reaction of the hydroxyl group on lamivudine with the carboxyl group on various polymers.[11] The polymers incorporate several sites of activity including the lamivudine to modify the control release of the lamivudine. Most of the current efforts focus on simple compounding of lamivudine for control-release of the drug.[12-14]

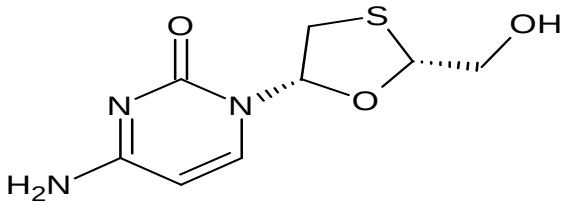

Fig 01: Structure of lamivudine.

Our initial biological assays focus on the ability of the polymers to inhibit human cancer cell lines. Along with the anticancer and antibacterial activity of organotin polymers, they also have exhibited antiviral activity. This has been recently reviewed.[1][5][15] We have synthesized other polymers containing the amine and alcohol groups, namely poly(amine ethers). Most notably of these are polymers from acyclovir.[5][17] The inhibitory activity of acyclovir is highly selective.[17] Acyclovir is widely used to inhibit several herpes viruses, particularly HSV-1 and HSV-2. It is also used to treat varicella-zoster virus (VZV), Epstein-Barr virus (EBV), and the cytomegalovirus (CMV). Thus, acyclovir is a first line

antiviral drug. A variety of polymers were synthesized using acyclovir as the Lewis base focusing attention on organotin materials with respect to their antiviral activity (Fig.2).[5][17] Results of antiviral studies showed that many of the polymers out performed acyclovir itself.

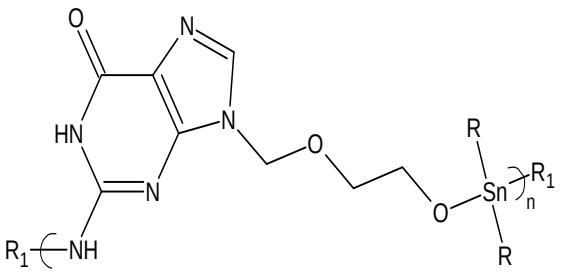

Fig. 02: Repeat unit for the product derived from reaction of acyclovir with organotin dihalides.

Eventually we plan to study the antiviral activity of the organotin polymers containing lamivudine hoping to inhibit other unwanted pathogens, the present focus in on inhibition of cancer.

The biological activity of organotin compounds has been known for over one hundred years.[1-6][16] For over 80 years their ability to inhibit cancer growth has also been known. In fact, more organotin compounds have undergone testing as possible anticancer materials than any other single group of compounds.[5][16] Finally, commercially there are more different organotin compounds available than any other metal-containing organometallic.[5][16]

Here we describe the synthesis, structural characterization, and preliminary ability to inhibit the cell growth of a battery of human cancer cell lines. The overall structure of the polymer is described in Fig. 3 for the dimethyltin product.

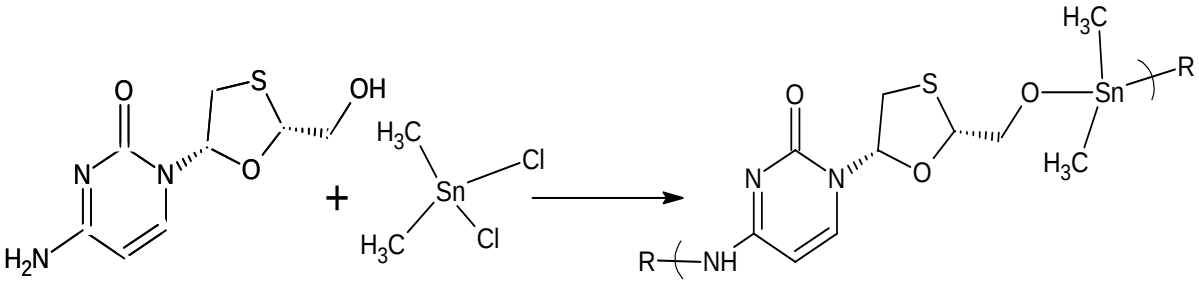

Fig 03: Synthesis of organotin polymer containing lamivudine where R is simply chain extension.

EXPERIMENTAL

Synthesis

The following reactants were used as received: diphenyltin dichloride (1135-99-5), dimethyltin dichloride (753-73-1) and dibutyltin dichloride (683-18-1) were purchased from Aldrich Chemical Co., Milwaukee, WS; diethyltin dichloride (866-55-7) was obtained from Peninsular Chemical Res., Gainesville, FL; dioctyltin dichloride (3542-36-7) was obtained from Ventron Alfa Inorganics, Beverly, Mass., and lamivudine (134678-17-4) from Cambridge Chemicals, Woburn, Mass.

Reactions were carried out using the interfacial polycondensation technique. Briefly, an aqueous solution (30 ml) containing the lamivudine (0.00300 mol) and sodium hydroxide ((0.0060 mol) was transferred to a one-quart Kimax emulsifying jar fitted on top of a Waring Blender (model 1120; no load speed of about 18,000 rpm; reactions were carried out at about 25^{o}C). Stirring was begun and a heptane solution (30 ml) containing the organotin dihalide (0.00300 mol) was rapidly added (about 3-4 seconds) through a hole in the jar lid using a powder funnel. The resulting solution was blended for 15 seconds. Solid formed almost instantaneously. The precipitate was recovered using vacuum filtration and washed several times with deionized water and heptane to remove unreacted materials and unwanted by-products. This process effectively removed unreacted heptane since its presence was not found in the spectral analysis of the products. The solid was washed onto a glass petri dish and allowed to dry at room temperature.

Structural Characterization

Light scattering photometry was carried out in DMSO employing a Brice-Phoenix Universal Light Scattering Photometer Model 4000. Infrared spectra were obtained employing attenuated total reflectance infrared spectroscopy utilizing a JASCO FT/IR-4100 fitted with an ATR Pro 450-s. ^{1}H NMR spectra were obtained employing Varian Inova 400 MHz and Varian 500 MHz spectrometers. High resolution electron impact positive ion matrix assisted laser desorption ionization time of flight, HR MALDI-TOF, mass spectrometry was carried out employing a Voyager-DE STR BioSpectrometer, Applied Biosystems, Foster City, CA. The standard settings were used with a linear mode of operation and an accelerating voltage of 25,000 volts; grid voltage 90% and an acquisition mass range of 500 to 100,000. Fifty to two hundred shots were typically taken for each spectrum. Results employing graphite are included in the present paper. Addition of graphite was accomplished by simply "drawing" on the matrix sample holder assembly and placing the powered polymer sample on top of the graphite drawing.

Cell Testing

The toxicity of each test compound was evaluated against a battery of cancer cell lines. Following a 24 h incubation period, the text compounds were added at concentrations ranging from 0.0032 to 32,000 ng/mL and allowed to incubate at 37°C with 5% CO_2 for 72 h. Following incubation, Cell Titer-Blue reagent (Promega Corporation) was added (20 microL/well) and incubated for 2 h. Fluorescence was determined at 530/590 nm and converted to % cell viability versus control cells.

All cytotoxicity values are calculated against a base-line value for each line that was generated from "mock-treatment" of the normal and tumor cell lines with media supplemented with all diluents used to prepare the chemotherapeutic compounds. For example, if the compounds were dissolved in DMSO and serial dilutions prepared in Modified Eagle's Medium, MEM, to treat the cells, then the mock-treated cells were "treated" with the same serial dilutions of DMSO without added chemotherapeutic compound. This was done to ensure that any cytotoxicity observed was due to the activity of the compound and not the diluents. For the studies reported here, the mock-treatment never resulted in a loss of cell viability of more than one percent, demonstrating that the activity observed was not due to cytotoxicity of any of the diluents used, but was due to activity of the tested compounds. Once inhibition begun, the slope of the inhibition verses concentration was steep ending with total inhibition.

RESULTS AND DISCUSSION

Yields and Chain Lengths

Table 1 contains the product yield, molecular weight and chain length (degree of polymerization, DP) for the products.

Table 01: Product yield, molecular weight and chain length (DP) as a function of organotin moiety for the reaction of organotin dihalides with lamivudine.

Lamivudine	%-Yield	Molecular Weight	Chain Length
Organotin			
Me_2Sn	37	1.8×10^5	475
Et_2Sn	87	1.5×10^5	370
Bu_2Sn	94	1.0×10^5	220
Oc_2Sn	99	3.3×10^5	575
Ph_2Sn	93	4.5×10^5	900

Yield increases as the alkyl chain length increases in length. This may be due to the solubility of the organotin in the organic layer with the solubility increasing as the chain length increases. But as the alkyl chain length increases it becomes less polar and less soluble in the aqueous layer. For instance, the dimethyltin dichloride is the least soluble in the organic layer consistent with it being retained in the organic layer for a lesser relative time so that it enters the reaction zone more rapidly and exposed to the aqueous phase undergoing more rapid hydrolysis resulting in a lowered yield.

Infrared Spectral Results

The infrared spectral results appear in Table 2 for the dibutyltin and diphenyltin products and reactants. The assignments for lamivudine are based on literature assignments.[18] Organotin and connective assignments are also based on literature assignments.[15][17][19-23]

Bands characteristic of the presence of the various CH vibrations for both the organotin moiety and derived from lamivudine are found (all bands given in cm^{-1}). Additional bands are given in Table 2.

Table 02: Assigned peaks for the monomers and associated polymers derived from reaction with lamivudine and dibutyltin dichloride and diphenyltin dichloride.

Band Assignment	Lamivudine	Bu_2SnCl_2	Bu_2Sn/ Polymer	Ph_2SnCl_2	Ph_2Sn/ Polymer
O-H st	3934				
NH_2 asym st	3771				
NH_2 sym st	3645				
CH aromatic				3068,3051	3065,3050
C-H st	2915		2914		2913
CH_3 asym st		2959	2953		
CH_2 asym st		2926	2930		
CH_3 sym st		2872	2871		
CH_2 sym st		2858	2855		
C=O st	1651		1640		1638
C-H st	1497		1498		1495
Sn-Ph st				1480	1480
C=C st				1432	1428
CH st combo	1286		1288		1288
Sn-O asy st			1276		1275
Sn-Ph st				1071	1075
C-H twist, O-H st comb	1182,1161				
C-C st		1178,1152	1187,1158		
NH_2 st,N-C-N asym st	1088,1061				
C-O st, C-C st, C-H op st combo	1034		1030		1023
C-H bend, C-C st	918		917		918
Ring deformations	895,852, 806,789		893,860, 802,781		895,862, 800,785
CH_3 rock		878	873		
Sn-O sym st			781		771
Sn-N			722		719
Sym op bend H's				729	725

The band associated with simple O-H stretching about 3400 is missing as expected because of the formation of the Sn-O linkage. Bands associated with NH_2 stretching at 3771 and 3645 are now moved downfield, to about 3500 and 3230, again as expected because these are now associated with the formation of the Sn-NH- linkage and loss of one amine proton. Other bands associated with the influence in combination bands of the NH_2 and OH are missing or moved (such as bands at 1182, 1161, 1088, 1061). New bands associated with the formation of the Sn-O grouping and for the formation of the Sn-N linkage are found consistent with the formation of the polymer linkages between the lamivudine and the organotin moiety. These appear about 780 for the Sn-O and 720 for Sn-N.

NMR Spectroscopy

^{1}HNMR assignments for lamivudine are consistent with those reported in literature.[24,25] Assignments for the organotin compounds are also consistent with those reported in literature.[16][18-22]

The ^{1}HNMR of the product of dibutyltin dichloride and lamivudine shown in Fig. 4 shows major peaks that correspond with both lamivudine and dibutyltin. The first major peak, located furthest downfield, is located at 7.88 ppm. The peak is split into a doublet and has an integration of 1H. This peak represents the hydrogen adjacent to the nitrogen heteroatom in the pyrimidinone ring. The second major peak is located at 5.75 ppm. The peak is split into a doublet and has the peak integration of 1H. This peak denotes the hydrogen three bonds away from the nitrogen atoms in the pyrimidinone ring. The third major peak is located at 6.15 ppm. The peak is split into a triplet with an integration of 1H. This peak represents the hydrogen on the oxathiolane ring adjacent to the nitrogen on the aromatic ring. The next peak major peak is located at 5.16 ppm. The peak is split into a triplet and has the peak integration of 1H. This peak represents the hydrogen adjacent to sulfur and oxygen on the oxathiolane ring. The next peak major peak is located at 3.73 ppm. The peak is split into a multiplet, has an integration of 2H and represents the hydrogens adjacent to the oxathiolane ring. The next major peaks are located at 3.39 and 3.01 ppm. The peaks are both split into doublet of doublets and have peak integrations of 1H. These peaks represent diasteriotopic hydrogen on the oxathiolane ring. The next major peak corresponds to the methylene hydrogens on the dibutyl groups the peak at 1.50 ppm i**s** **s**pilt into a multiplet and has a peak integration of 8H. The next major peak is located at 1.23 ppm it is split into a triplet and has an integration of 6H. This peak represents the terminal hydrogens on the butyl group. The final peak located furthest upfield appears at

0.82 ppm it is split into a multiplet and has an integration of 4H. This peak represents the hydrogens on the butyl group adjacent to tin.

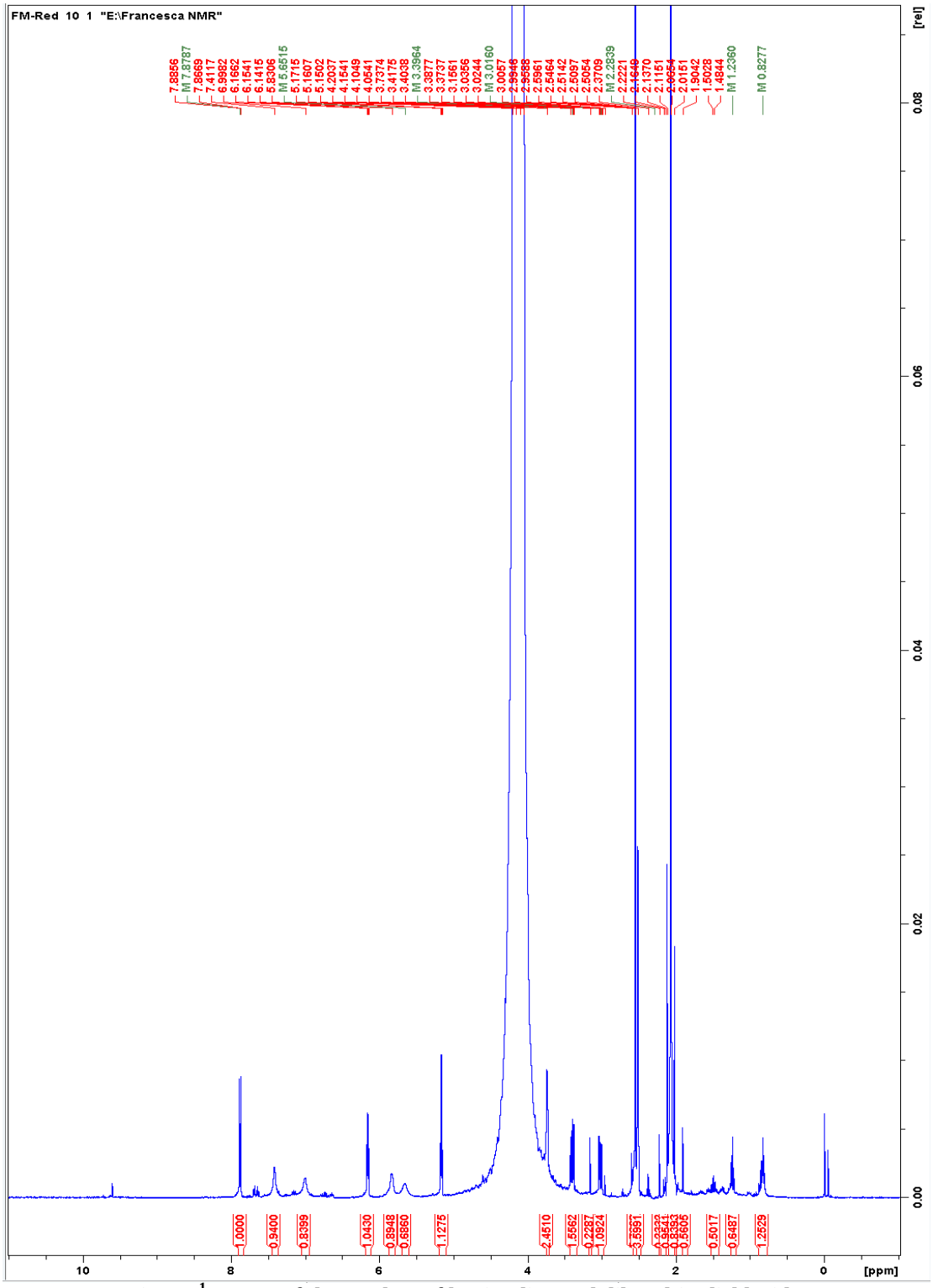

Fig.04: [1]HNMR of the product of lamivudine and dibutyltin dichloride.

The [1]HNMR of the product from dimethyltin dichloride lamivudine shown in Fig. 5 shows major peaks that correspond with both lamivudine and dimethyltin. The first major peak, located furthest downfield, is located at 7.92 ppm. The peak is split into a doublet and has an integration of 1H. This peak represents the hydrogen adjacent to the nitrogen heteroatom in the pyrimidinone ring. The second major peak is located at 5.88 ppm. The peak is split into a doublet and has the peak integration of 1H. This peak denotes the hydrogen three bonds away from the nitrogen atoms in the pyrimidinone ring. The third major peak is located at 6.18 ppm. The peak is split

into a triplet with an integration of 1H. This peak represents the hydrogen on the oxathiolane ring adjacent to the nitrogen on the aromatic ring. The next peak major peak is located at 5.20 ppm. The peak is split into a triplet and has the peak integration of 1H. This peak represents the hydrogen adjacent to sulfur and oxygen on the oxathiolane ring. The next peak major peak is located at 3.78 ppm. The peak is split into a multiplet, has an integration of 2H and represents the hydrogens adjacent to the oxathiolane ring. The next major peaks are located at 3.40 and 3.05 ppm. The peaks are both split into doublet of doublets and have peak integrations of 1H. These peaks represent diasteriotopic hydrogen on the oxathiolane ring. The final major peak corresponds to the hydrogens on the dimethyl groups the peak at 0.64 ppm is spilt into a singlet and has a peak integration of 6H.

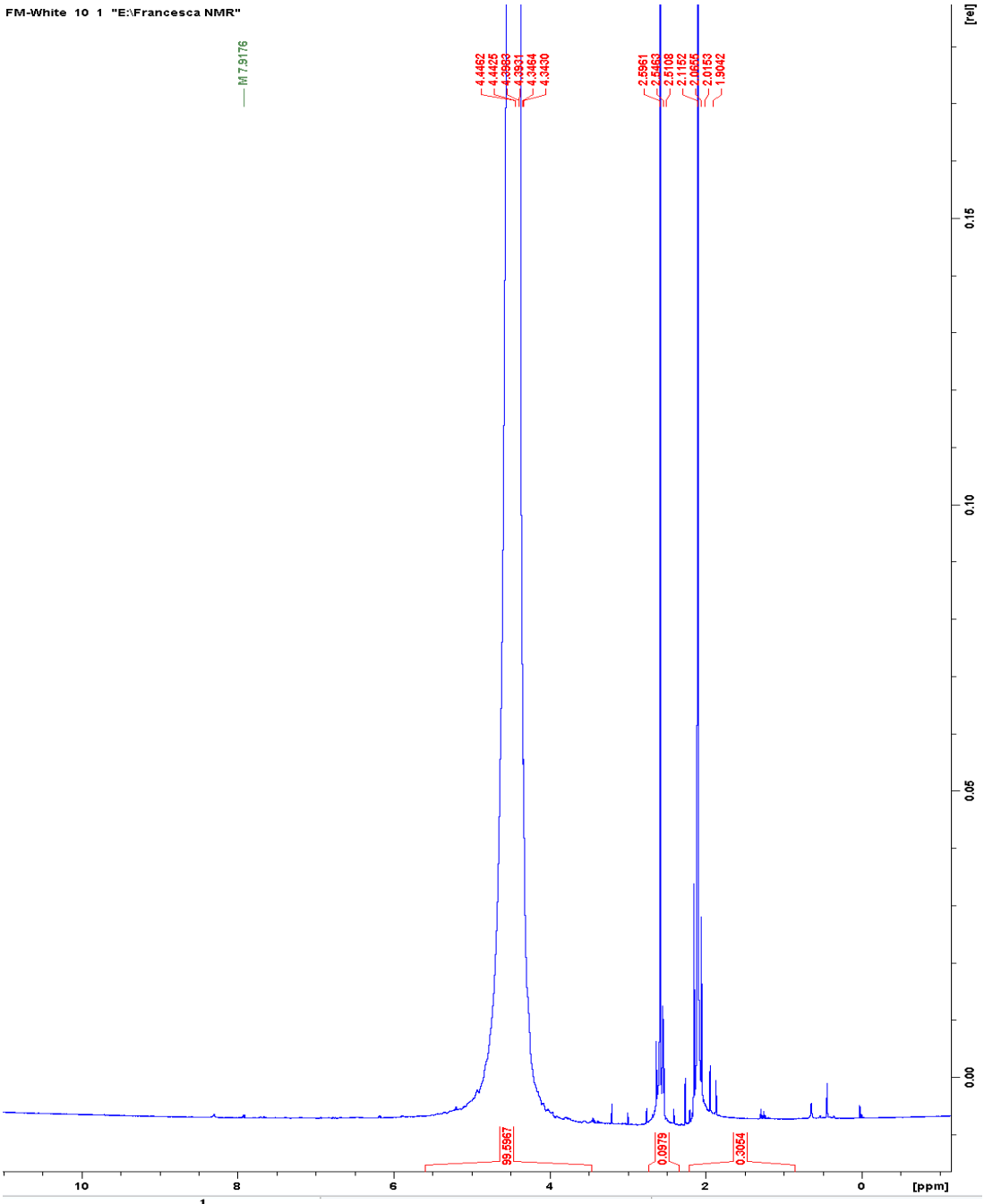

Fig 05: [1]HNMR of the product of lamivudine and dimethyltin dichloride.

The [1]HNMR of the product from dioctyltin dichloride and lamivudine shown in Fig. 6 shows major peaks that correspond with both lamivudine and dioctyltin. The first major peak, located furthest downfield, is located at 7.89 ppm. The peak is split into a doublet and has an integration of 1H. This peak represents the hydrogen adjacent to the nitrogen heteroatom in the pyrimidinone ring. The second major peak is located at 5.82 ppm. The peak is split into a doublet and has the peak integration of 1H. This peak denotes the hydrogen three bonds away from the nitrogen atoms in the pyrimidinone ring. The third major peak is located at 6.16 ppm. The peak is split

into a triplet with an integration of 1H. This peak represents the hydrogen on the oxathiolane ring adjacent to the nitrogen on the aromatic ring. The next peak major peak is located at 5.16 ppm. The peak is split into a triplet and has the peak integration of 1H. This peak represents the hydrogen adjacent to sulfur and oxygen on the oxathiolane ring. The next peak major peak is located at 3.74 ppm. The peak is split into a multiplet, has an integration of 2H and represents the hydrogens adjacent to the oxathiolane ring. The next major peaks are located at 3.40 and 3.02 ppm. The peaks are both split into doublet of doublets and have peak integrations of 1H. These peaks represent diasteriotopic hydrogen on the oxathiolane ring. The next major peak corresponds to the methylene hydrogens on the dioctyl groups the peak at 1.24 ppm i**s** **s**pilt into a multiplet and has a peak integration of 24H. The next major peak is located at 1.19 ppm it is split into a multiplet and has an integration of 6H. This peak represents the terminal hydrogens on the octyl group. The final peak located furthest upfield appears at 0.81 ppm it is split into a triplet and has an integration of 4H. These peaks represent the hydrogen atoms on the octyl groups adjacent to tin.

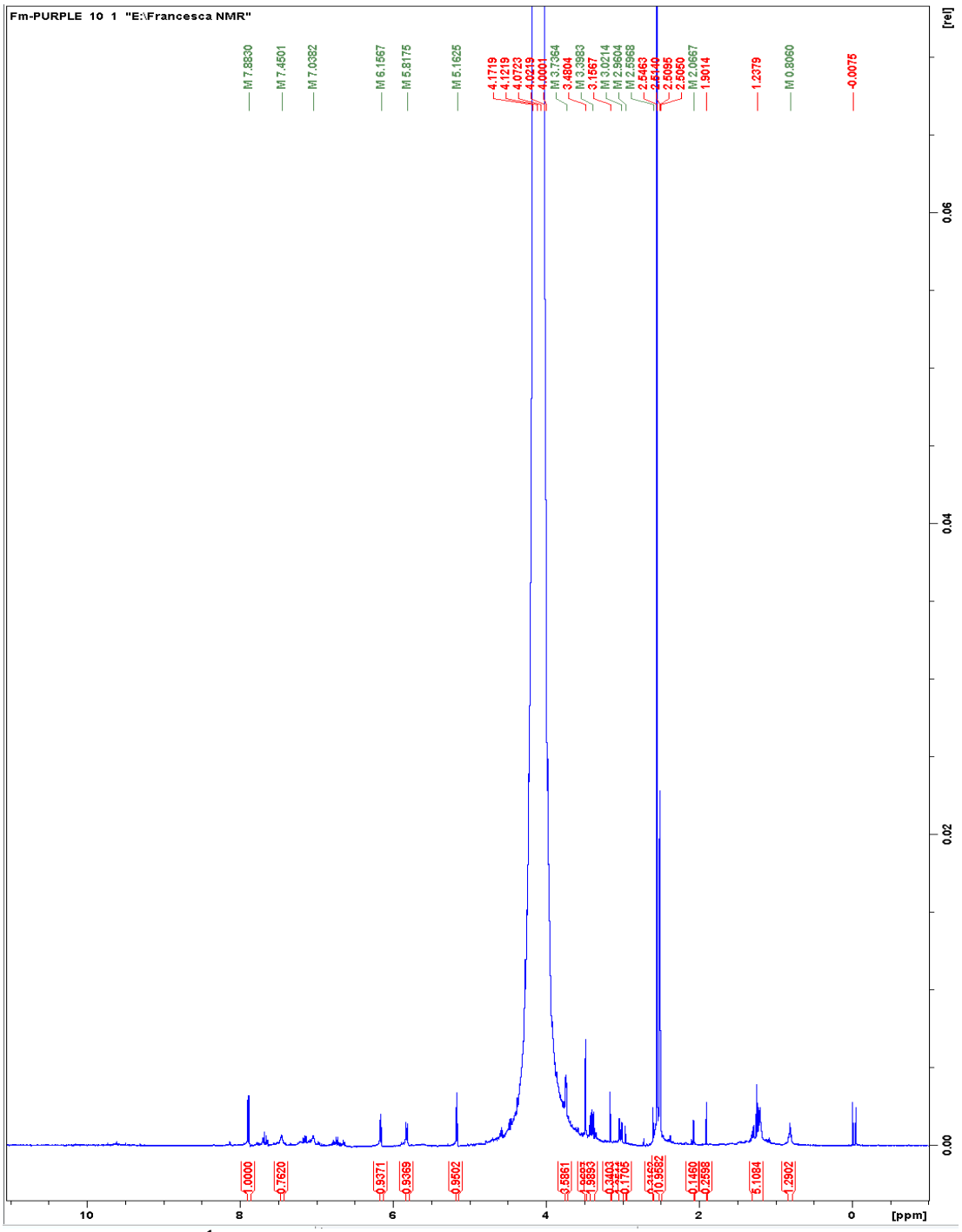

Fig 06: ^{1}HNMR of the product of lamivudine and dioctyltin dichloride.

The [1]HNMR of the product of diethyltin dichloride and lamivudine shown in Fig. 7 shows major peaks that correspond with both lamivudine and diethyltin. The first major peak, located furthest downfield, is located at 7.88 ppm. The peak is split into a doublet and has an integration of 1H. This peak represents the hydrogen adjacent to the nitrogen heteroatom in the pyrimidinone ring. The second major peak is located at 5.86 ppm. The peak is split into a doublet and has the peak integration of 1H. This peak denotes the hydrogen three bonds away from the nitrogen atoms in the pyrimidinone ring. The third major peak is located at 6.14 ppm. The peak is split into a triplet with an integration of 1H. This peak represents the hydrogen on the oxathiolane ring adjacent to the nitrogen on the aromatic ring. The next peak major peak is located at 5.16 ppm. The peak is split into a triplet and has the peak integration of 1H. This peak represents the hydrogen adjacent to sulfur and oxygen on the oxathiolane ring. The next peak major peak is located at 3.76 ppm. The peak is split into a multiplet, has an integration of 2H and represents the hydrogens adjacent to the oxathiolane ring. The next major peaks are located at 3.39 and 3.01 ppm. The peaks are both split into doublet of doublets and have peak integrations of 1H. These peaks represent diasteriotopic hydrogen on the oxathiolane ring. The next major peak corresponds to the methylene hydrogens on the diethyl groups the peak at 1.24 ppm i**s** **s**pilt into a multiplet and has a peak integration of 4H. The final peak located furthest upfield appears at 1.03 ppm it is split into a multiplet and has an integration of 4H. This peak represents the hydrogens on the ethyl group adjacent to tin.

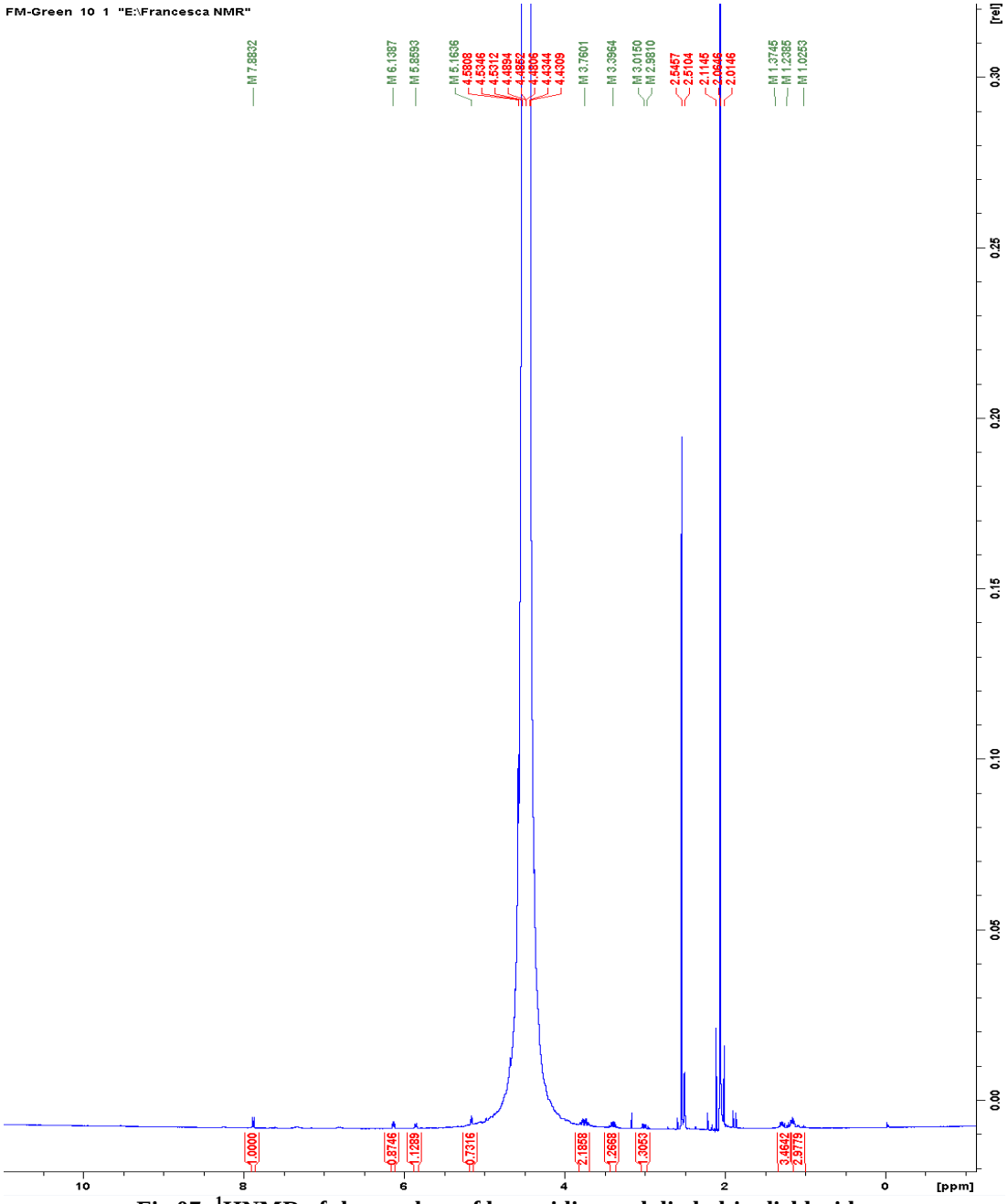

Fig 07: [1]HNMR of the product of lamuvidine and diethyltin dichloride.

The [1]HNMR of the product of diphenyltin dichloride and lamivudine shown in Fig. 8 shows major peaks that correspond with both lamivudine and diphenyltin. The first major peak, located furthest downfield, is located at 8.01 ppm. The peak is split into a doublet and has an integration of 1H. This peak represents the hydrogen adjacent to the nitrogen heteroatom in the pyrimidinone ring. The second major peak is located at 7.30 ppm, the peak is split into a multiplet and denotes the hydrogens on the phenyl rings of the phenyltin associate moiety. The third major peak is located at 5.91 ppm. The peak is split into a doublet and has the peak integration of 1H. This peak denotes the hydrogen three bonds away from the nitrogens in the pyrimidinone ring. The fourth major peak is located at 6.15 ppm. The peak is split into a triplet with an integration of 1H. This peak represents the hydrogen on the oxathiolane ring adjacent to the nitrogen on the aromatic ring. The next peak major peak is located at 5.18 ppm. The peak is split into a triplet and has the peak integration of 1H. This peak represents the hydrogen adjacent to sulfur and oxygen on the oxathiolane ring. The next peak major peak is located at 3.77 ppm. The peak is split into a multiplet, has an integration of 2H and represents the hydrogens adjacent to the oxathiolane ring. The final major peaks are located at 3.43 and 3.08 ppm. The peaks are both split into doublet of doublets and have peak integrations of 1H. These peaks represent diasteriotopic hydrogen on the oxathiolane ring.

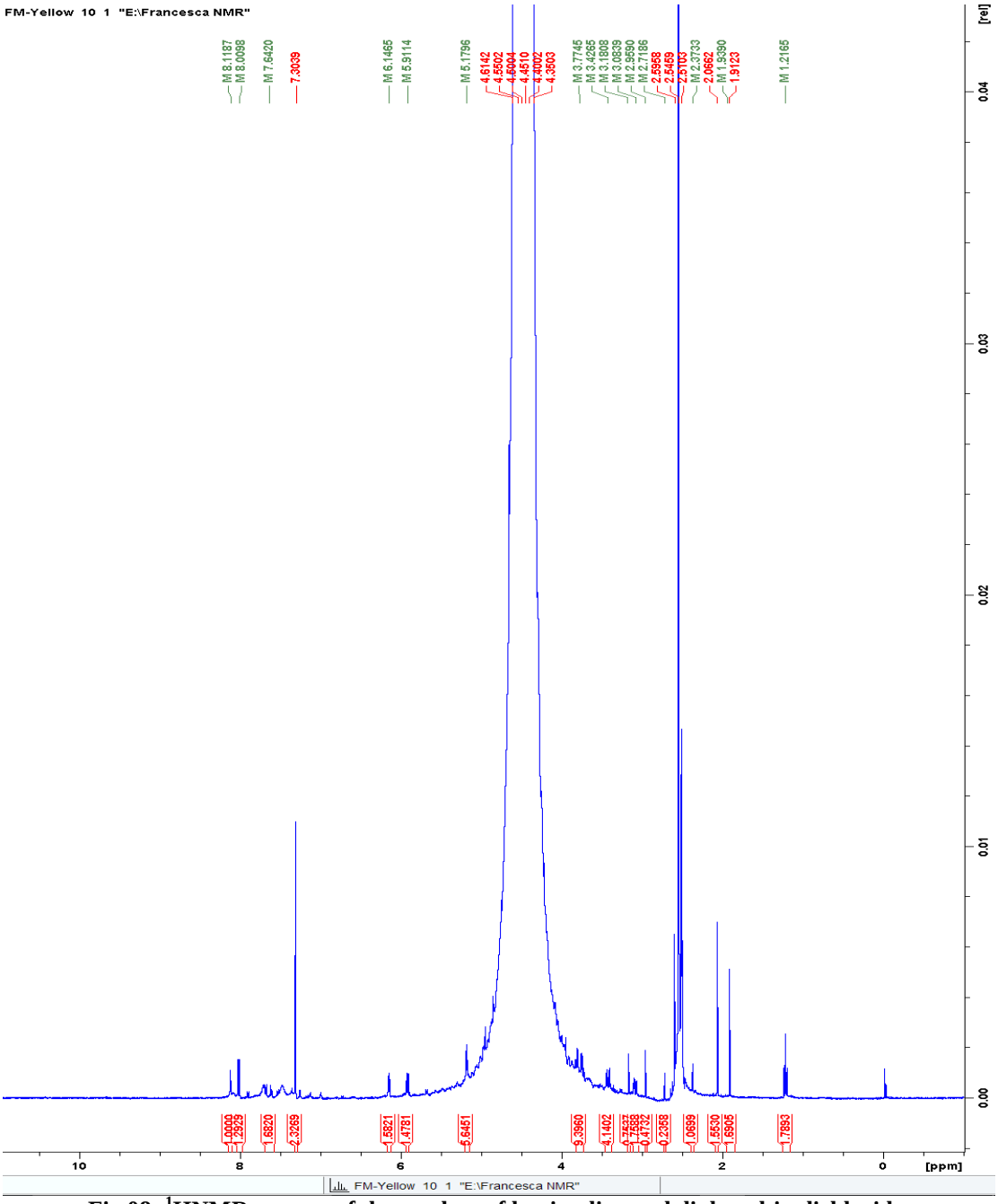

Fig 08: [1]HNMR spectra of the product of lamivudine and diphenyltin dichloride.

The nmr spectra shows the expected absence of the acid-associated proton and one of the amine protons consistent with formation of the linking bonds. The second amine proton is also absent as expected due to exchanging with the solvent in this case dimethyl sulfoxide, DMSO. It also shows the presence of organotin and lamivudine associated bands as expected.

Matrix Assisted Laser Assisted Desorption Ionization Mass Spectroscopy MALDI MS

The solid-state fragmentation of various polymers employing MALDI MS emphasizing metal-containing polymers for use in the structural identification of these polymers has been studied by us. General MALDI MS analysis of synthetic polymers has been largely curtailed because of the requirement that both the matrix and polymer must be soluble in readily volatile liquids that allow intimate mixing of the matrix and polymer. We have employed a modification of this technique that allows MALDI MS to be obtained on non-volatile and insoluble products. This approach has been recently reviewed.[26,27] In this approach, the focus in on the ion fragments created from the degradation of the polymer backbone.

MALDI MS spectra were obtained for the monomers and polymers. Recently we have been employing graphite as the matrix material because it gives good results with few interfering ion fragments produced above 500 Da mass which is the typical lower mass employed in our studies.[28-30]

MALDI MS bond cleavage typically occurs at heteroatoms within the polymer backbone. For the lamivudine moiety three observed units are usually created with one derived from lamivudine itself and two from breakage at the internal nitrogen creating two moieties that are described as the pyrimidine, P, portion and the second the thiacytidine, S, portion designated as such in the following tables.

Fig. 09 contains the MALDI MS for the product derived from the reaction of dibutyltin dichloride and lamivudine. Table 3 contains assignments of ion fragment clusters derived from this polymer. Ion fragment clusters to nine units are found over the range of 500 to 5,000 Da. The following abbreviations are employed to describe these ion fragment clusters: Sn for the $SnBu_2$, L is the lamivudine minus two protons, P for the pyrimidine portion, S for the thiacytidine portion, Bu the butyl group, U for one repeat unit, 2U for two repeat units, etc. Sodium, Na, is a common contaminant.

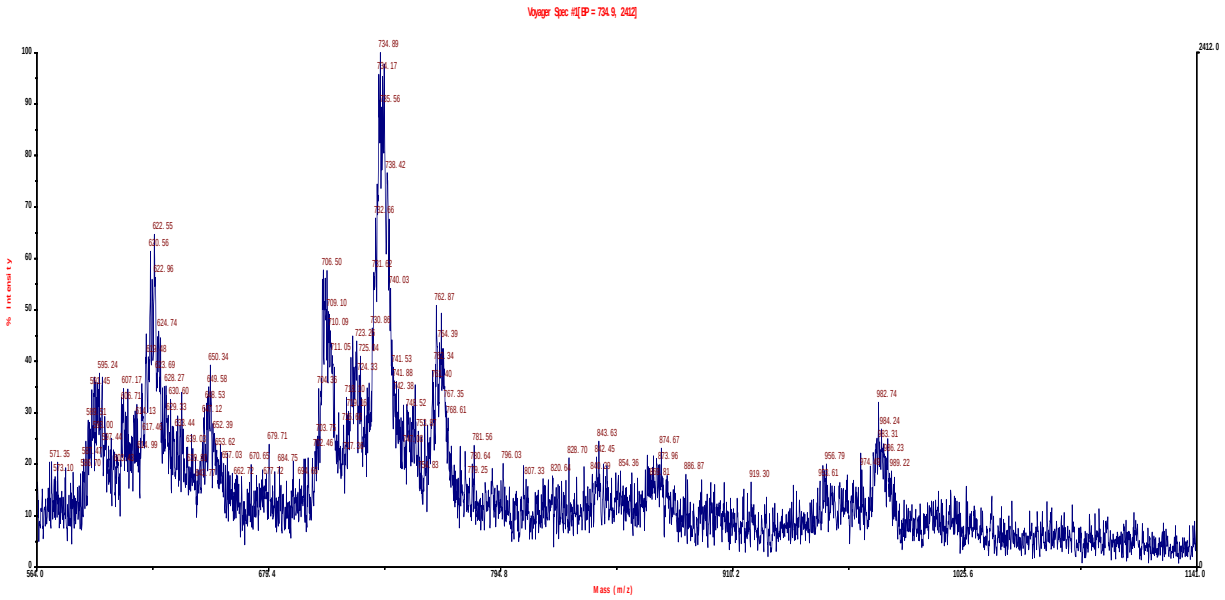

Fig 09: MALDI MS of the product of dibutyltin dichloride and lamivudine over the approximate range of 550 to 1100 Da.

Table 03: Major ion fragment clusters for the product of dibutyltin dichloride and lamivudine.

Mass, Da	(Tenative) Assignment
571	U+P
595	U+P,Na
623	U+T,O,Na
706	U+Sn,NH
735	U+Sn,O,Na
763	U+Sn, 2O,Na
844	U+Sn,P,O,Na
868	2U-Bu
1017	2U+P-O
1079	2U-Bu,O
1146	2U+L
1252	2U+Sn,P-NH
1372	3U-O
1476	3U+P-NH
1520	3U+T,Na
1576	3U+O,Sn-Bu
1707	3U+Sn,P-NH
1914	4U+P-Bu
2061	4U+Na-NH
2210	4U+Sn,P,Na
2436	5U+P,Na
2626	5U+Sn,P-NH
2810	6U+O,Na
3010	6U+Sn,NH
3186	7U-O,Bu
3384	7U+L-Bu,O
3593	7U+Sn,P,Na
3804	8U+T
4102	9U-Bu

Tin has ten isotopes of which seven are present in amounts greater than 5 %. The presence and relative abundance of these isotopes in ion fragment clusters is employed to confirm the presence/absence of tin within the ion fragment clusters. The relative intensities form a type of "fingerprint" that can be visually identified. Fig. 7 contains a number of these fingerprint regions. These regions can be further studied in tabular form comparing the observed relative ion intensities found in the MALDI MS of the samples compared to the relative abundance observed in nature for tin isotopes. Tables 4 and 5 contain such matches for ion fragments containing one and two tin atoms. The agreement with the known relative abundances is reasonable consistent with the presence of tin atoms in the ion fragment clusters. At higher masses, isotope matches are difficult because of the low intensities of generated ion fragments.

Table 04: Isotopic abundance matches for two tin-containing ion fragment clusters containing one tin atom (only ion fragments >5% relative abundance are reported) for the product of dibutyltin dichloride and lamivudine.

Known for Sn		U+P,Na		U+T,O,Na	
116	45	590	42	619	46
117	24	591	28	620	26
118	75	592	72	621	75
119	26	593	30	622	32
120	100	594	100	623	100
122	14	596	15	625	16
124	17	598	18	627	18

Table 05: Isotopic abundance matches for three tin-containing ion fragment clusters containing two tin atoms (only ion fragments >5% relative abundance are reported) for the product of dibutyltin dichloride and lamivudine.

Known for Sn		U+Sn,NH		U+Sn,O,Na		U+Sn,2O,Na	
232	12	701	14	729	14	758	14
233	13	702	15	730	16	759	15
234	43	703	40	731	45	760	44
235	35	704	36	732	40	761	40
236	94	705	96	733	100	762	100
237	51	706	62	734	63	763	58
238	100	707	100	735	100	764	100
239	35	708	35	736	34	746	36
240	81	709	82	737	84	766	83
242	32	711	35	739	34	768	34
244	22	713	25	741	25	768	25

Fig. 10 contains the MALDI MS for the analogous diethyltin dichloride product. The tin isotopic abundance fingerprints are present. Table 6 contains major ion fragments for the diethyltin dichloride/lamivudine product over the mass range of 500 to 5000 Da. Again, the major bond scission occurs at the non-carbon atoms within the polymer chain. Ion fragment clusters to ten units are found. Similar abbreviations as employed in Table 8 are used but where Et represents the ethyl moiety.

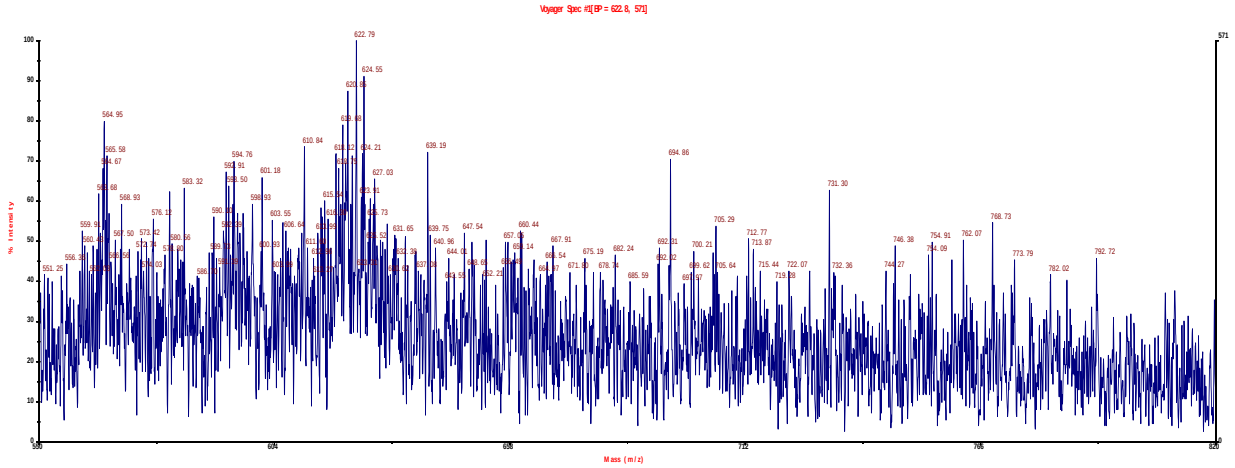

Fig 10: MALDI MS of the product of diethyltin dichloride and lamivudine of the approximate range of 550 800 Da.

Table 06: Major ion fragment clusters for the product of dibutyltin dichloride and lamivudine.

Mass, Da	(Tenative) Assignment
545	U+Sn
556	U+Sn-Et
567	U+Sn,O-Et
579	U+Sn
597	U+Sn,O
615	U+Sn,2O
626	U+L
663	U+Sn,P-Et
697	U+Sn,P
719	U+Sn,T,O
734	U+Sn,P,O,Na
792	2U-NH
854	2U+O,Na
911	2U+P
982	2U+Sn
1063	2U+L,Na
1186	3U-Bu
1302	3U+P-O
1404	3U+Sn,NH
1424	3U+Sn,2O
1481	3U+Sn,P-NH
1519	3U+Sn,P,O
1552	3U+Sn,T,O
1607	4U-NH
1769	4U+Sn-2O
1839	4U+L
1921	4U+Sn,T
1930	4U+Sn,P,Na
2362	5U+Sn,O,Na
2423	6U
2560	6U+P,Na
2731	6U+Sn,P,O
2931	7U+P-O
3064	7U+L
3896	9U+Sn,P-2O
3953	9U+Sn,P,Na
4319	10U+Sn,P-O

Table 07: Isotopic abundance matches for two tin-containing ion fragment clusters containing two tin atoms (only ion fragments >5% relative abundance are reported).

Known for Sn		2U+L		2U+Sn,P-Et	
232	12	620	15	657	15
233	13	621	16	658	16
234	43	622	44	659	40
235	35	623	40	660	36
236	94	624	93	661	90
237	51	625	52	662	52
238	100	626	100	663	100
239	35	627	36	664	32
240	81	628	82	665	74
242	32	630	34	667	37
244	22	632	24	669	22

Isotopic abundance matches for two ion fragment clusters each containing two tin atoms is given in Table 7. The isotopic matches are in reasonable agreement with the standard and consistent with the presence of two tin atoms in the fragment clusters.

As noted before, for the present lamivudine polymers the major bond scission creating the observed ion fragment clusters occur at the non-carbon atoms as indicated in fig. 11 for the dimethyltin polymer repeat unit.

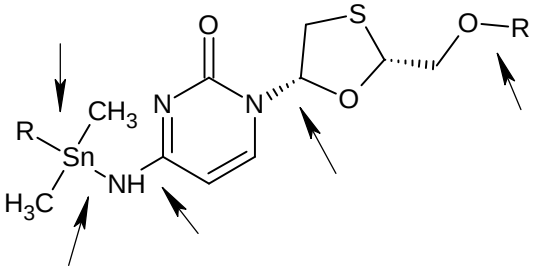

Fig 11: Sites of major bond scission for the lamivudine polymers, here for the repeat unit from dimethyltin moiety.

Cancer Cell Lines

As noted before, a major purpose in synthesizing metal-containing polymers is to investigate their ability to inhibit unwanted pathogens and infectious agents. Here the focus is cancer. Table 8 contains the cell lines employed in the current study.

Table 08: Cell lines employed in the current study.

Strain Number	NCI Designation	Species	Tumor Origin	Histological Type
3465	PC-3	Human	Prostate	Carcinoma
7233	MDA MB-231	Human	Pleural effusion breast	Adenocarcinoma
1507	HT-29	Human	Recto-sigmoid colon	Adenocarcinoma
7259	MCF-7	Human	Pleural effusion-breast	Adenocarcinoma
ATCC CCL-75	WI-38	Human	Normal embryonic lung	Fibroblast
CRL-1658	NIH/3T3	Mouse	Embryo-continuous cell line of highly contact-inhibited cells	Fibroblast
	U251	Human	Glioblastoma multiforme	Astrocytomas
	G55	Human	Glioblastoma	Astrocytomas
	AsPC-1	Human	Pancreatic cells	Adenocarcinoma
	PANC-1	Human	Epithelioid pancreatic cells	Carcinoma

The two most widely used approaches employed to evaluate cell line data are used in the present study. The first approach measures the concentration dose needed to reduce the growth of the particular cell line. The term effective concentration, EC, is used here. The amount of a tested material that induces inhibition halfway between the baseline and maximum is referred to as the 50% response concentration and given the symbol EC_{50}. EC_{50} values for the monomers and polymers, including values for cisplatin as a standard, are given in Table 9. Cisplatin is a widely used anticancer drug. It is toxic as indicated by the low EC_{50} values for the two standard cell lines, NIH 3T3 and WI-38. In combating cancer cisplatin, and other related platinum drugs, exhibit many unwanted side effects in patients including loss of hair, loss of taste, numbness, vomiting, kidney damage, hearing loss, etc.[31] Even so, it remains among the most widely employed drugs for the treatment of cancer.[31]

For the current study several observations are found. The EC_{50} for the polymers are significantly lower (more toxic) than for the lamivudine monomer. Also, the EC_{50} values for the polymers are lower compared with the organotin monomers. Thus, it is the combination of the Lewis acid/base, lamivudine/organotin, that is primarily responsible for the observed ability to inhibit cell line growth. For other studies as the organotin dihalide is varied for a Lewis base, the polymer containing the dibutyltin moiety typically shows the greatest ability to curtail cancer cell line growth followed by those containing the diphenyltin moiety.[4-8] This trend is found for a variety of Lewis acid/base pairs. For the current study, this general trend is also found so the best inhibition, lowest EC_{50}, is generally found for the dibutyltin polymer followed by the diphenyltin polymer. The observation that the dibutyltin polymers do exhibit decent inhibition of all the cancer cell lines is important since dibutyltin dichloride is the least expensive of the organotin halides and available in gram to ton amounts.[16] Because of its widespread commercial use, more is known about it than any of the other organotin monomers. It is the least toxic to humans of the organotin monomers. [16] Finally, in nature it degrades to simple tin oxide offering a low toxic form of degradation product. Even so, while it is widely employed as a paint additive, dibutyltin dichloride is required to be in polymeric form if it is used in marine coatings since it leeches and limits sea life growth in waterways.[16]

The following focuses on the ability of the polymers to inhibit specific cancer cell lines. There is no effective treatment of pancreatic cancer once it metastasizes. In the USA yearly about 32,000 new cases are diagnosed yearly. Within a year almost all patients die. Worldwide, it is the fourth leading cause of cancer death. We found that inhibition of pancreatic cancer cell lines is difficult compared with other human cancer cell lines (excepting brain cancer). Even so, we found a number of organotin polymers that exhibit good ability to inhibit pancreatic cancer. In the current study the two most widely studied human pancreatic cancer cell lines are used. The tested cell lines are AsPC-1 which is an adenocarcinoma pancreatic cell line, which accounts for about 80% of the diagnosed human pancreatic cancers, and PANC-1 which is an epithelioid carcinoma pancreatic cell line, accounting for about 10% of the human pancreatic cancer cases. In the current study, the organotin polymers show decent inhibition of both cell lines with the inhibition similar for the two cell lines. This similarity is consistent with the idea that the polymers may offer broad-spectra inhibition of other pancreatic cancer cell lines.

In the present study a matched pair of breast cancer cell lines were used. The MDA-MB-231 (strain number 7233) cells are estrogen-independent, estrogen receptor negative while the MCF-7 (strain line 7259) cells are estrogen receptor (ER) positive. In some other studies a major difference in the ability to inhibit these two cell lines by the organotin polymers was found.[32] When the Lewis base in the polymer contained an oxygen-phenylene grouping that connects the Lewis base to the organotin moiety such as hydroquinone and hydroquinone derivatives there was a major difference.

We believe this was due to the structural similarity present in drugs such as diethylstilbestrol that are employed as drugs in the treatment of breast cancer. The present polymers do not show such differentiation between the two types of breast cancer cell lines and do not show this structural similarity to such breast cancer drugs thought there is a Sn-O connection, the oxygen is not connected to an aromatic group.

Table 09: EC_{50} Concentrations (micrograms/mL) for the tested compounds derived from various organotin polymers, monomers, lamivudine and cisplatin. Values given in ( ) are Standard Deviations for each set of measurements.

Sample	3T3	*WI-38*	*PANC-1*	*AsPC-1*
Me_2SnCl_2	0.43 (.1)	0.22(.1)	0.80(.1)	0.71(.1)
Me_2Sn/LA	0.33(.05)	0.37(.05)	0.41(.05)	0.38(.05)
Et_2SnCl_2	0.46(.1)	0.20(.1)	0.48(.1)	0.90(.1)
Et_2Sn/LA	0.35(.05)	0.36(.05)	0.42(.05)	0.42(.05)
Bu_2SnCl_2	0.20 (.05)	0.20(.05)	0.0032(.001)	0.012(.01)
Bu_2Sn/LA	0.31(.05)	0.37(.05)	0.34(.05)	0.40(.05)
Oc_2SnCl_2	0.56(.1)	0.30(.1)	0.85(.1)	0.85(.1)
Oc_2Sn/LA	0.37(.05)	0.37(.05)	0.42(.05)	0.40(.05)
Ph_2SnCl_2	0.66(.1)	0.25(.1)	0.71(.1)	0.83(.1)
Ph_2Sn/LA	0.70(.05)	0.39(.05)	0.32(.05)	0.30(.05)
Lamivudine	1.6(.05)	1.7(.05)	1.6(.05)	1.6(.05)
Cisplatin	0.015(.01)	0.012(.01)	0.0023(.005)	0.0035(.005)

Sample	PC-3	MDA-MB-231	HT-29	MCF-7
Me_2SnCl_2	0.51(.1)	0.44(.1)	0.56(.1)	0.66(.1)
Me_2Sn/LA	0.37(.05)	0.37(.05)	0.37(.05)	0.33(.05)
Et_2SnCl_2	0.61(.1)	0.64(.1)	0.71(.1)	0.77(.1)
Et_2Sn/LA	0.37(.05)	0.32(.05)	0.30(.05)	0.41(.05)
Bu_2SnCl_2	1.4(1.1)	1.4(1.3)	1.2(.1)	0.70(.06)
Bu_2Sn/LA	0.39(.05)	0.33(.05)	0.33(.05)	0.37(.05)
Oc_2SnCl_2	0.55(.1)	0.65(.1)	0.65(.1)	0.70(.1)
Oc_2Sn/LA	0.33(.05)	0.32(.05)	0.30(.05)	0.33(.05)
Ph_2SnCl_2	0.82(.1)	0.76(.1)	0.56(.1)	0.68(.1)
Ph_2Sn/LA	0.31(.05)	0.32(.05)	0.32(.05)	0.34(.05)
Lamivudine	1.6(.05)	1.6(.05)	1.6(.05)	1.6(.05)
Cisplatin	0.0044(.004)	0.0029(.002)	0.0041(.003)	0.0057(.003)

Sample	*U251*	*G55*
Me_2SnCl_2	0.91(.5)	1.2(.6)
Me_2Sn/LA	0.49(.05)	0.55(.06)
Et_2SnCl_2	1.1(.6)	1.3(.6)
Et_2Sn/LA	0.65(.05)	0.74(.07)
Bu_2SnCl_2	1.0(.2)	1.0(.4)
Bu_2Sn/LA	0.44(.05)	0.47(.05)
Oc_2SnCl_2	1.3(.7)	0.95(.6)
Oc_2Sn/LA	O,61(.06)	0.63(.06)
Ph_2SnCl_2	0.89(.6)	0.97(.6)
Ph_2Sn/LA	0.67(.06)	0.62(.05)
Lamivudine	1.6(.05)	1.6(.05)
Cisplatin	0.015(.01)	0.020(.01)

Recently we begun to look at the ability of our polymers to inhibit the growth of human glioblastoma brain cancer. Like pancreatic cancer, the expected life expectancy once glioblastoma cancer is found is less than a year. The lamivudine polymers are one of the initial compounds tested and results are given in Table 11. G55 is a relatively new human glioblastoma cell line. It was developed by C. David James (Department of Neurological, University of California and San Francisco. It is a human glioblastoma cell line that had been passed through nude mice and re-established as a stable xenograft cell line. The U251 cell line is one of the most used cancer cell lines. It is derived from a human malignant glioblastoma multiforme. Astrocytomas are brain cancer that originates in astocytes. High-grade astocytomas, called glioblastoma multiforme, are the

most malignant of all brain tumors. Studies involving various cancer cell lines show that the G55 cells tend to be more invasive more accurately modeling brain cancer because of this greater invasiveness and migration since they form invasive intracranial tumors in rodents more characteristic of primary human glioblastoma multiforme, GBM. There is no decent chemo treatment for brain cancer thus the ability to inhibit it by treatment with chemo drugs is greatly needed. The current organotin polymers show ability to inhibit both types of brain cancer cell lines (Table 9). The inhibition is better, generally lower EC_{50}, for the polymers compared with the organotin monomers and lamivudine.

The second calculation for measuring anticancer effectiveness is called the chemotherapeutic index, CI, where the CI_{50} is the ratio of the EC_{50} for the standard cell line NIH/3T3 or WI-38 cells divided by the EC_{50} for the test cell. These results are shown employing WI-38 cells as the standards in Table 10. Values greater than one are desirable in this measure since it indicates that there is a preference for inhibiting the cancer cell lines in comparison to the standard cells. In the present case, there are no CI_{50} values greater than one. On the positive side, most CI_{50} values for the polymers are greater than those of the monomers.

Table 10: CI_{50} values for monomers and polymers derived from data given in Table 11 based on WI-38 data.

Sample	EC_{50}WI-38/ EC_{50}PNC-1	EC_{50}WI-38/ EC_{50}AsPC-1	EC_{50}WI-38/ EC_{50}PC-3	EC_{50}WI-38/ EC_{50}MDA
Me_2SnCl_2	0.28	0.31	0.43	0.50
Me_2Sn/LA	0.90	1.0	1.0	1.0
Et_2SnCl_2	0.83	0.81	0.91	0.91
Et_2Sn/LA	0.86	0.86	0.97	1.1
Bu_2SnCl_2	63	18	0.14	0.14
Bu_2Sn/LA	1.1	0.93	0.97	1.1
Oc_2SnCl_2	0.35	0.35	0.55	0.46
Oc_2Sn/LA	0.88	0.93	1.1	1.2
Ph_2SnCl_2	0.35	0.31	0.30	0.33
Ph_2Sn/LA	1.2	1.3	1.3	1.2
Cisplatin	5.2	3.4	2.7	4.1

Sample	EC_{50}WI-38/ EC_{50}MCF-7	EC_{50}WI-38/ EC_{50}HT-29	EC_{50}WI-38/ EC_{50}U251	EC_{50}WI-38/ EC_{50}G55
Me_2SnCl_2	0.39	0.39	0.45	0.31
Me_2Sn/LA	1.1	1.0	0.76	0.67
Et_2SnCl_2	0.71	0.67	0.34	0.29
Et_2Sn/LA	0.88	1.2	0.55	0.49
Bu_2SnCl_2	O,29	0.17	0.33	0.33
Bu_2Sn/LA	1.0	1.1	0.84	0.79
Oc_2SnCl_2	0.43	0.46	0.34	0.46
Oc_2Sn/LA	1.1	1.2	0.61	0.79
Ph_2SnCl_2	0.37	0.45	0.29	0.30
Ph_2Sn/LA	1.2	1.2	0.58	0.63
Cisplatin	2.1	2.9	0.80	0.57

The two cell lines most used as standards are the NIH/3T3 and WI-38 cell lines. NIH/3T3 cells are mouse embryo fibroblast cells. They are part of a group of cell lines that are referred to as partially transformed cells in that they are immortal unlike normal cells. They retain other characteristics of normal cells such as being contact-inhibited. Relative to most normal cells they are robust and easily maintained. WI-38 cells are normal embryonic human lung fibroblast cells. They have a finite life time of about 50 replications. Compared to NIH/3T3 cells, they are more fragile and difficult to maintain for long periods of time. While NIH/3T3 cells are often favored because of ease of handling aided by an infinite life span, results from WI-38 cells are given greater importance when there is a difference.[1-6] Table 11 contains the CI_{50} values based on the WI-38 standard human cell line.

Thus, the current polymers show good inhibition of the cancer cell lines based on EC_{50} values, they do not show outstanding ability to differentiate cancer cell line growth based on CI_{50} values. There is not agreement as to whether the EC_{50} or CI_{50} values are most significant in the evaluation of cancer inhibition. Thus, results for both are presented.

SUMMARY

Organotin poly(amine ethers) were rapidly synthesized in good yield employing the interfacial polycondensation system. The synthesis employed commercially available reactants allowing for possible production in gram to ton

quantities. Infrared spectroscopy showed the formation of new bands characteristic of the Sn-O- and Sn-N linkages. MALDI MS and NMR results are consistent with the proposed structure with ion fragment clusters to ten units. Proton NMR results are consistent with the proposed repeat unit. The polymers exhibit good inhibition of all of the tested human cancer cell lines including two human brain glioblastoma cancer cell lines, two human pancreatic cancer cell lines and two human breast cancer cell lines based on EC_{50} values.

Author contributions

Structural analysis and synthesis-F. Mosca, C. Carraher, P. Slawek, J. Haky.

Biological analysis-M. Roner, L. Miller, A. Moric-Johnson.

Conflicts of Interest

None.

REFERENCES

1. Roner M.R., Carraher C.E., Shahi K, Barot G., Antiviral Activity of Metal-Containing Polymers—Organotin and Cisplatin-Like Polymers, Materials, 2011; 4: 991-1021.
2. Carraher C.E., Siegmann-Louda D., Organotin macromolecules as anticancer drugs, in Macromolecules Containing Metal and Metal-Like Elements, Vol 3. Biomedical Applications, Wiley, 2004.
3. Carraher C.E., Organotin macromolecules as anticancer drugs in Macromolecules containing metal and metal-like elements, NJ, John Wiley & Sons, 2004.
4. Carraher C.E., Roner M.R., Organitin Polyethers as Biomaterials, Materials, 2009; 2: 1558-1598.
5. Carraher C.E., Roner M.R., Organotin Polymers as Anticancer and Antiviral Agents, Journal of Organometallic Chemistry, 2013; 751: 67-82.
6. Carraher C.E, Organotin polymers, Wiley, Hobokin, 2005.
7. Cohen J., Powderly W., Opal S., Infectious Diseases, NY, Elsevier, 2017.
8. Paintsil E., Chen Y.C., Antiviral Agents, NY, Elsevier, 2009.
9. Kimberlin D., Laboratory Diagnosis and Therapy of Infectious Diseases, NY, Elsevier, 2012.
10. Pandey G, Yadav S.K, Mishra B., Preparation and characterization of isoniazid and lamivudine co-loaded polymeric microspheres, Artif Cells Nanomed Biotechnol, 2016; 44: 1867-1877.
11. Danial M., Andersen A.H., Zuwala K., Cosson S., Riber C.F., Smith A.A., Tolstrup M., Moad G., Zelikin A.N., Postma A., Triple Activity of Lamivudine Releasing Sulfonated Polymers against HIV-1, Mol Pharm, 2016; 13(7): 2397-2410.
12. Sandhiya V., Rama B., Srishna K., Dhanani U., Dhunmathi K., Preparation and Characterization of Chitosan Loaded Nanoparticles for Anti-Viral Drug, World J. Pharm. and Pharmaceutical Sciences, 2016; 5: 721-730.
13. Naresh Y., Baru C., Vidyahara S., Sasidhar R., Formulation Design and Characterization of Matrix Tablets of Lamivudine, Indo Am. J. Pharmaceutical Sciences, 2015; 2(1): 514-522.
14. Song B., Puskas I., Szente L., Hildreth J.E.K., Hyaluronic Acid-Based Biocompatible Supramolecular Assembly for Sustained Release of Antiretroviral Drug, J Pharm Sci, 2016; 105: 2760-2769.
15. Roner M.R., Carraher C.E., Roehr J.L., Bassett K.D., Antiviral and anticancer activity of organotin polymers and reactants derived from norfloxacin and ampicillin, Journal of Polymer Materials, 2006; 23: 153-159.
16. Hoch M., Organotin Compounds in the Environment-anoverview, Applied Geochemistry, 2001; 16: 719-743.
17. Carraher C.E., Sabir T.S., Roner M.R., Shahi K., Bleicher R.E., Roehr J.L, Bassett K.D., Synthesis of organotin polyamine ethers containing acyclovir and their preliminary anticancer and antiviral activity, Journal of Inorganic and Organometallic Polymers and Materials, 2006; 16: 249-257.
18. Du Y., Zhang H., Xue J., Tang W., Fang H., Zhang Q., Li Y., Hong Z., Raman and tetahertz spectroscopic investigation of cocrystal formation involving antibiotic nitrofurantion drug and coformer 4-aminobenzoic acid, Spectrochim Acta A Mol Biomol Spectrosc, 2015; 137: 1158-1163.
19. Carraher C., Roner M.R., Islam Z., Moric-Johnson A., Group 15 Organotin Containing Polyamines from Histamine and Their Ability to Inhibit Cancer Cell Lines from Pancreatic, Breast and other Cancers, J. Pharmacy & Pharmacetical Res., 2018; 2: 1.
20. Carraher C.E., Roner M.R., Moric-Johnson A., Miller L., Barot G., Sookdeo N., Ability of Simple Organotin Polyethers to Inhibit Pancreatic Cancer, J. Macromol. Sci., 2016; 53: 63-71.
21. Carraher C.E., Roner M.R., Chrichton R., Moric-Johnson A., Miller L., Black K., Russell F., Synthesis and Preliminary Cancer Cell Line Results for the Product of Organotin Dihalides and Alpha-Cyano-4-Hydroxycinnamic Acid, Journal of Inorganic and Organometallic Polymers and Materials, 2016; 26: 1351-.
22. Carraher C.E., Roner M.R., Lynch M., Moric-Johnson A., Miller L., Slawek P., Mosca F, Frank J., Organotin Poly(ester ethers) from Salicylic Acid and Their Ability to Inhibit Selected Human Cancer Cell Lines, Journal of Clinical Research in Onology, 2018; 1: 1-11.
23. Carraher C.E., Truong N.T.C., Roner M.R., Synthesis of Metallocene Poly(ether Esters) from Reaction of Group IVB and VB Metallocene Dichlorides with Glycyrhetinic Acid, J. Polym. Mater., 2017; 34: 435-454.

24. Kurmi M., Sahu A., Singh D.K., Singh I.P., Singh S., Stability behaviour of antiretroviral drugs and their combinations. 8: Characterization and in-silico toxicity prediction of degradation products of efavirenz, J Pharm Biomed Anal, 2018; 148: 170-181.
25. Roy P., Nigam N., Singh M., George J., Srivastava S., Naqvi H., Shukla Y., Tea polyphenols inhibit cyclooxygenase-2 expression and block activation of nuclear factor-kappa B and Akt in diethylnitrosoamine induced lung tumors in Swiss mice, Invest New Drugs, 2010; 28: 466-471.
26. Carraher C.E., Barot G., Battin A., Reactions Between the Matrix and Ion Fragments Created from the MALDI MS of Organotin-Containing Polymers, Journal of Polymer Materials, 2009; 26: 17-31.
27. Carraher C.E., Sabir T.S., Carraher C., Fragmentation matrix assisted laser desorption/ionization mass spectrometry-basics, Journal of Polymer Materials, 2006; 23: 143-151.
28. Carraher C.E., Sabir T., Carraher C.L, Fundamentals of Fragmentation Matrix Assisted Laser Desorption/Ionization Mass Spectrometry, NY, Springer, 2008.
29. Carraher C.E., Suresh V., Roner M.R., Self Matrix Activity of Organotin Polyether Ester Polymers Containing Alpha-Cyano-4-Hydroxycinnamic Acid, JCAMS, 2015; 3: 32-44.
30. Carraher C.E., Roner M.R., Carraher C.L., R. Crichton, and K. Black, Use of Mass Spectrometry in the Characterization of Polymers Emphasizing Metal-Containing Condensation Polymers, J. Macromol. Sci., 2015; 52(11): 867-886.
31. Oun R., Moussa Y.E., Wheate N.J., The side effects of platinum-based chemotherapy drugs: a review for chemists, Dalton Trans, 2018; 47: 6645-6653.
32. Carraher C.E., Roner M.R., Shahi K., Barot G., Structural Consideration in Designing Organotin Polyethers to Arrest the Growth of Breast Cancer Cells *In Vitro*, Materials, 2011; 4: 801-815.